J. Fluid Mech. (2010), *vol.* 646, *pp.* 441–451.
doi:10.1017/S0022112009993144

Localized edge states nucleate turbulence in extended plane Couette cells

TOBIAS M. SCHNEIDER[1,2], DANIEL MARINC[1,3] AND BRUNO ECKHARDT[1,4]†

[1]Fachbereich Physik, Philipps-Universität Marburg, D-35032 Marburg, Germany

[2]School of Engineering and Applied Sciences, Harvard University, Cambridge, MA 02138, USA

[3]Aerodynamisches Institut, RWTH Aachen, D-52062 Aachen, Germany

[4]Department of Mechanical Engineering, TU Delft, 2928 CA Delft, The Netherlands

(Received 3 September 2009; revised 30 October 2009; accepted 31 October 2009)

We study the turbulence transition of plane Couette flow in large domains where localized perturbations are observed to generate growing turbulent spots. Extending previous studies on the boundary between laminar and turbulent dynamics we determine invariant structures intermediate between laminar and turbulent flow. In wide but short domains we find states that are localized in spanwise direction, and in wide and long domains the states are also localized in downstream direction. These localized states act as critical nuclei for the transition to turbulence in spatially extended domains.

1. Introduction

In fluids heated from below (Rayleigh–Bénard convection) or in centrifugally unstable situations (Taylor–Couette flow) (Koschmieder 1993) the transition to turbulence proceeds through sequences of bifurcations that add spatial and temporal degrees of freedom to the flow until eventually the complex spatio-temporal dynamics which characterizes turbulent motion is reached. Such a scenario, similar in spirit to the ideas of Landau (1944) but different in detail, does not apply to several important flows like pressure driven flow down a circular pipe (Reynolds 1883) or plane Couette flow (Schmid & Henningson 1999; Eckhardt *et al.* 2007), since already the first step of the classical scenario, the linear instability of the laminar profile, is missing. Accordingly, triggering turbulence in these linearly stable flows requires that both the flow rate *and* the strength of an applied perturbation exceed critical levels (Boberg & Brosa 1988; Grossmann 2000). Several experimental (Darbyshire & Mullin 1995; Dauchot & Daviaud 1995; Bottin *et al.* 1998; Hof, Juel & Mullin 2003; Peixinho & Mullin 2007) and numerical studies (Schmiegel & Eckhardt 1997; Meseguer 2003; Schneider, Eckhardt & Yorke 2007; Eckhardt *et al.* 2008) have focused on the required minimal perturbations and have identified a very sensitive dependence of the critical amplitudes on both the spatial structure of a perturbation and on the flow rate.

From a dynamical systems point of view, the coexistence of the stable laminar profile with turbulent dynamics implies that there is a boundary in the state space of

† Email address for correspondence: bruno.eckhardt@physik.uni-marburg.de

the system which separates perturbations that return to the laminar profile from those that become turbulent (Eckhardt *et al.* 2002, 2007). The sensitive dependence on initial conditions results in a fractal and convoluted boundary which was termed *edge of chaos* (Skufca, Yorke & Eckhardt 2006; Schneider *et al.* 2007; Vollmer, Schneider & Eckhardt 2009). It generalizes the more familiar basin boundary to situations where turbulence seems to be transient (Hof *et al.* 2006). Despite its intricate geometry the edge is locally formed by the stable manifold of an invariant dynamical object called *edge state*. By definition, the edge state corresponds to a self-sustained non-laminar and non-decaying flow field of critical energy. Its stable manifold is of codimension one per construction and defines locally the stability boundary. Therefore, the edge state together with its stable manifold determines minimal seeds for turbulence.

Both the exact solutions that have been linked to turbulent dynamics (Nagata 1990; Clever & Busse 1997; Waleffe 2003; Eckhardt *et al.* 2008) and the edge states (Wang, Gibson & Waleffe 2007; Duguet, Willis & Kerswell 2008; Schneider *et al.* 2008) which guide the transition have been studied in small computational domains subject to periodic boundary conditions. Thus, they focus on the temporal degrees of freedom but cannot capture large scale spatial phenomena such as the growth of turbulent regions or the coexistence of turbulent and non-turbulent patterns observed in spatially extended systems. The spatial dynamics of extended flow systems shows up in transition experiments where the homogeneously driven flow is locally perturbed by a jet injection (Bottin *et al.* 1998) or a small obstacle (Bottin, Dauchot & Daviaud 1997): in such cases one first observes a localized turbulent region which then starts to spread out (Emmons 1951). The spatially extended edge states cannot explain these phenomena, since they would require that the perturbation exceeds the critical threshold everywhere in space, in contrast to the experimental evidence. Studies on pipe flow, both in a model (Willis & Kerswell 2009) and in the fully resolved direct numerical simulations (Mellibovsky *et al.* 2009) have identified an edge state that is localized along the axis. In the present study we apply these ideas and tools to the case of plane Couette flow, where there are two directions of spatial extension, streamwise and spanwise. Using direct numerical simulations we show that these edge states can be localized in one or both directions, thereby confirming the expectation that a localized perturbation should be sufficient to nucleate turbulence. Moreover, we find tantalizing similarities to observations in typical pattern forming systems (Knobloch 2008). During the completion of this work we became aware of related studies by Duguet, Schlatter & Henningson (2009).

2. Edge states in wide Couette systems

As usual, we define the Reynolds number for plane Couette flow as $Re = u_0 d/\nu$, where u_0 is half the velocity difference between the two plates, d is half the gap width and ν the viscosity of the fluid. In the following all lengths will be given in units of d. The system is translationally invariant in both the streamwise (x) and spanwise (z) direction. The laminar linear flow profile is stable against infinitesimal perturbations for all Re (Schmid & Henningson 1999). In the turbulent case the translational symmetries are broken: localized turbulent patches of irregular shapes and various sizes which are surrounded by laminar regions can be observed for Re above about 320 (Bottin *et al.* 1998). The system also allows for more ordered patterns of turbulent stripes which arise for a small range of parameters near $Re = 400$ and were reproduced in numerical simulations (Prigent *et al.* 2002; Barkley & Tuckerman 2005). For these

Re localized perturbations are observed to generate localized turbulent spots that invade the surrounding laminar flow (Bottin *et al.* 1998).

As in previous studies in small periodic domains, we determine the edge state by numerically tracking the evolution of velocity fields which neither become fully turbulent nor decay to laminar flow but remain in regions intermediate between these two types of dynamics (Itano & Toh 2001; Skufca *et al.* 2006; Schneider *et al.* 2007; Vollmer *et al.* 2009). For the numerical simulation we use the Fourier–Chebyshev-tau scheme (Canuto *et al.* 1990) as implemented by Gibson (2004) with a resolution of 33 modes in normal direction. In the other directions, we adjust the number of modes when varying the size of the domain so that we keep $16/\pi$ modes per length in the spanwise and $4/\pi$ or $8/\pi$ modes per length in the downstream direction. With these numbers of modes the energy in the modes drops below 10^{-5} times the maximal value at about two-thirds of the highest wavenumbers. Moreover, with the asymmetric choice of resolution in spanwise and streamwise direction the energies for comparable mode numbers are similar (see Marinc 2008). One might expect that computing *localized* edge states requires a control not only on the perturbation energy but also on the spatial extension of a flow structure. However, as became clear in hindsight and will be demonstrated below, the evolution of these states is such that no additional control is needed and that the numerical algorithm described before (Schneider *et al.* 2008; Schneider & Eckhardt 2009) can be used without modification.

A domain that is 2π wide and 4π long suffices to support turbulent dynamics and is close to optimal for the appearance of coherent structures (Clever & Busse 1997; Waleffe 2003). We first focus on $Re = 400$, keep the length of the reference domain fixed and extend its width to 8π and then 16π. In contrast to the case of the small domain, where a non-localized state has been found, the edge tracking algorithm now converges to a state that is localized in the spanwise direction, as shown in figure 1(*b*). This state is not symmetric under reflection on the mid-plane and hence is not stationary but a travelling wave that moves with a phase speed c_x of $6.9 \times 10^{-3} u_0$ downstream. There exists a reflected partner travelling in the opposite direction. In the core region the state is dominated by pairs of downstream vortices that induce alternating high- and low-speed streaks. The topology is similar to the three-dimensional state described by (Nagata 1990; Clever & Busse 1997; Waleffe 2003) and the non-localized edge state in small domains (Schneider *et al.* 2008), reproduced here periodically repeated for the wider domain in figure 1(*c*). The state in figure 1(*a*) is a stationary localized state discussed further below.

The eigenvalue spectrum shown in figure 2(*a*) confirms the conclusion drawn from the convergence of the edge state tracking, namely that the stable manifold is of codimension one. The variation of the total energy content with the box width shown in figure 2(*b*) confirms the localization properties: the energy first increases but then settles to an essentially constant value once the width exceeds 7π. This confirms that the properties are intrinsically controlled by the dynamics and not induced by the boundaries.

Using a Newton method, the travelling waves can be pinned and followed to different Reynolds numbers. The kinetic energy in figure 3(*a*) and the spanwise size as determined from a Gaussian fit, $\propto \exp(-x^2/\sigma^2)$, in figure 3(*b*) show that the solution is spatially extended for low *Re*, localizes as *Re* increases and reaches a constant width beyond $Re \approx 250$. The state's phase velocity (figure 3*c*) first deviates from zero at $Re \approx 150$ and oscillates with *Re*. The next to leading eigenvalue is shown in figure 3(*d*): its real part becomes negative for *Re* slightly above 200 and confirms

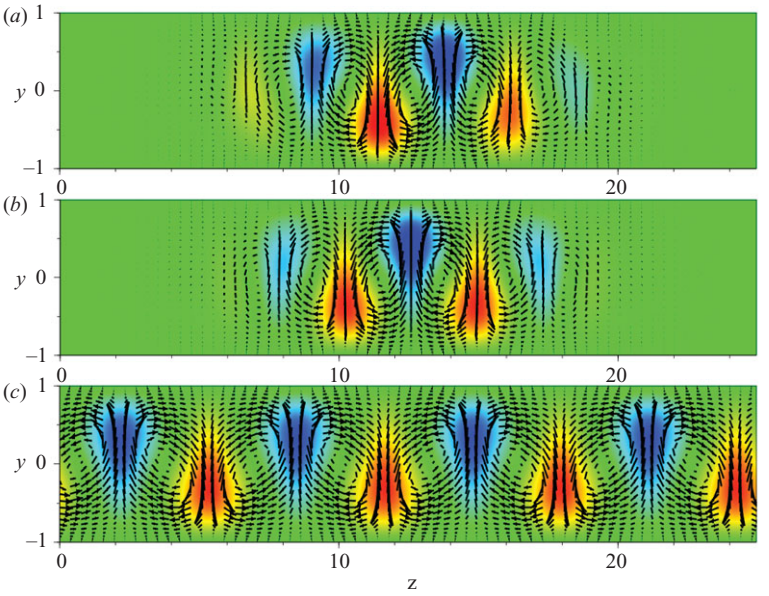

FIGURE 1. Symmetric (a), antisymmetric (b) and extended state (c) in plane Couette flow for $Re = 400$. Shown are downstream averages of the in-plane velocity components (arrows) and the downstream component (colour coded relative to the mean profile, blue regions are slower, red regions faster than the mean profile). The range of the velocity components reflected in the colours and lengths of arrows are $-0.7 < u_x < 0.7$, $-0.019 < u_y < 0.019$, and $-0.062 < u_z < 0.062$. (a) The velocity field that is symmetric with respect to a rotation around the centre and therefore corresponds to a stationary state. (b) The velocity field that is reflection symmetric along a line $z = const$, but not along a line $y = 0$. It does not represent a stationary state but a travelling wave. (c) The periodically continued edge state obtained from smaller domains. Note that the spanwise wavelength of the localized state is a bit shorter than the one for the extended state.

that the stable manifold of the travelling wave is of codimension one and that it is an edge state.

The presence of two locally attracting travelling waves on the edge calls for an explanation of how their stable manifolds and the two local boundaries between laminar and turbulent dynamics which they define can be sewed together. The simplest explanation (following the bifurcation scenarios discussed by Vollmer *et al.* 2009) requires the existence of a relative saddle in the edge which has an unstable direction pointing to either of the states. The broken up–down symmetry of the travelling waves then suggests that such a state should be symmetric. A Newton search starting from a suitably tailored initial condition indeed converges to the symmetric and stationary state shown in figure 1(a). Its eigenvalue spectrum shows the second unstable eigenvalue required to connect it to the travelling waves via a symmetry breaking bifurcation. Indeed, following both the travelling wave and the stationary state down to a Reynolds number close to 150.2, they merge. However, when approaching this point, the widths of the states increase (cf. figure 3), until they extend over the full domain near the bifurcation point. This is documented in figure 4, where we characterize the states using a specially tailored measure of the energy content. The quantity Σ is calculated from the energy difference between the state and its mirror image in the spanwise direction so that it amplifies the difference between the two localized states and shows the reduction in energy when they become localized.

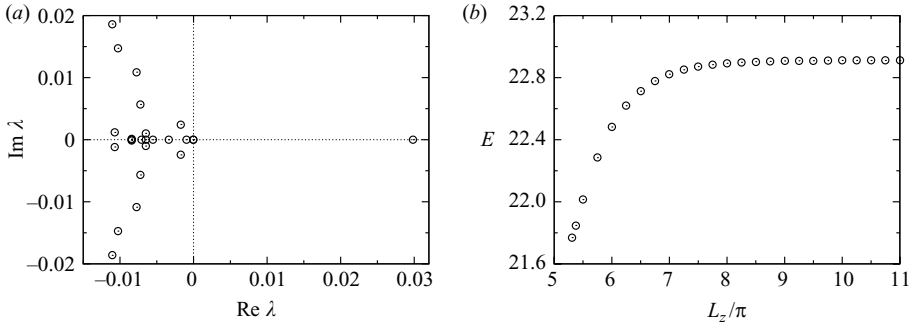

FIGURE 2. Properties of the edge state at $Re = 400$. (*a*) $\mathrm{Re}\,\lambda$ and $\mathrm{Im}\,\lambda$, the real and imaginary parts of the eigenvalues. One finds one unstable eigenvalue with positive real part, two neutral eigenvalues $\lambda = 0$ related to the continuous translational symmetries in downstream and spanwise direction and several stable real and complex eigenvalues. (*b*) The energy of the edge state as a function of the domain width L_z: the approach of a constant value for sufficiently large L_z indicates the converge to a state that is independent of the width L_z.

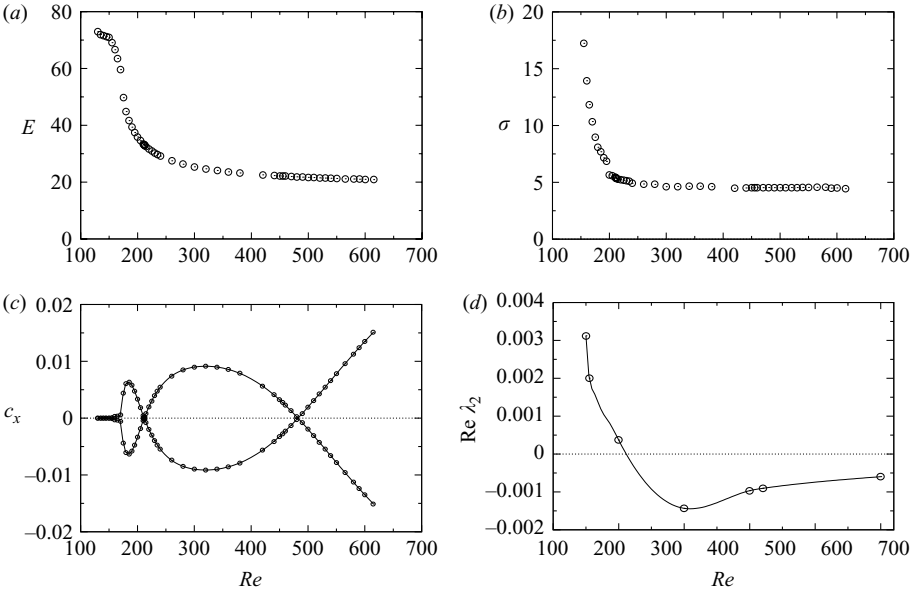

FIGURE 3. Properties of edge state for different Reynolds numbers *Re*. (*a*) The energy and (*b*) the width σ in a Gaussian approximation to the envelope $\propto \exp(-x^2/\sigma^2)$. Both quantities approach constants for *Re* above about 250. (*c*) The phase velocity c_x; it oscillates with *Re* and vanishes near $Re = 220$ and 480. The upper and lower curve belong to symmetry related states. (*d*) The real part of the next to leading eigenvalues λ_2. It crosses from unstable (for small *Re*) to stable (for larger *Re*) near $Re = 200$. The data points are connected by lines to guide the eye.

One notes that as the Reynolds number is reduced, all three solutions converge near $Re = 150.2$, showing that both the symmetric and antisymmetric localized state emerge out of the spatially extended equilibrium.

Similar localization phenomena have been observed in homoclinic snaking scenarios (Burke & Knobloch 2007; Knobloch 2008; Dawes 2009). The similarities in phenomenology are remarkable, and become particularly clear when the flow

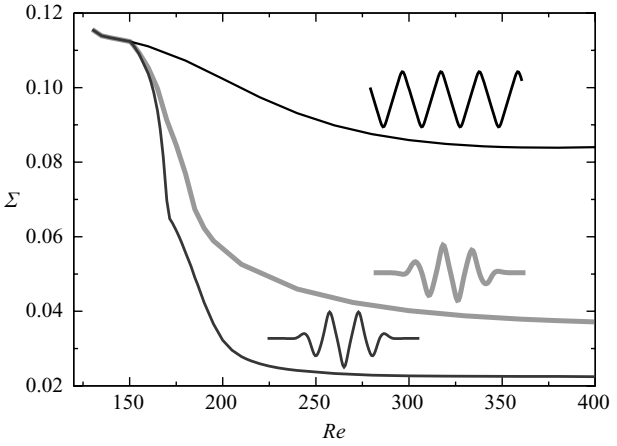

FIGURE 4. Bifurcation diagram for the localized travelling wave and the stationary state. The projection is defined by $\Sigma = \langle \vec{u}^2 \rangle_{x,y,z} - 12 \langle | \langle \vec{u}^2 \rangle_{x,z}(y) - \langle \vec{u}^2 \rangle_{x,z}(-y) | \rangle_y$. The different states are indicated with profiles of the z-dependent downstream velocities, averaged in downstream and wall-normal direction.

variations in downstream direction are averaged out and only the downstream velocities averaged in x and y are shown: According to the symmetries of the full three-dimensional velocity fields the averaged velocities come in patterns of either reflection or a point mirror symmetry, as shown in the profiles next to the curves in figure 4. Remarkably, the localized patterns in the one-dimensional Swift–Hohenberg model with cubic-quintic nonlinearity show the same symmetries (Burke & Knobloch 2007; Knobloch 2008; Dawes 2009). We also noticed that the states in the Swift–Hohenberg model and the ones obtained here can be scaled and superimposed to look almost identical: while such a quantitative agreement cannot be expected because of the different form of the equations from which they are obtained, it does underline the strong similarities between the two systems, thereby pointing to a similar localization mechanism.

3. Edge states in wide and long domains

Turning to domains that are 2π wide but much longer than 4π we find edge states that are localized in the downstream direction. However, their length falls off rather slowly, so that for $Re = 400$, where the length is about 60–80, boxes of a length 64π had to be used before localization could be seen (Marinc, Schneider & Eckhardt 2009). As in the wide box this edge state is dominated by streaks but it is neither a fixed point nor a travelling wave but shows constant internal dynamics similar to the chaotic edge state found in pipe flow (Schneider *et al.* 2007). Also the localization in downstream direction is not unlike the one seen in models and in full numerical simulations for pipe flow (Willis & Kerswell 2009; Mellibovsky *et al.* 2009).

Increasing both the width and length of the computational domain to 128 times the area of the reference domain, the edge tracking algorithm converges to a structure that is fully localized in spanwise and streamwise direction. Figure 5(*a*) shows the localized state for a domain with $L_x = 64\pi$ and $L_z = 16\pi$. Most of the energy density of the perturbation is concentrated within a length of 20 and a width of 5 as measured by the variance of the averaged kinetic energy distribution. The visual appearance including the tails of the structures is a bit larger, about 80×20. The localized state

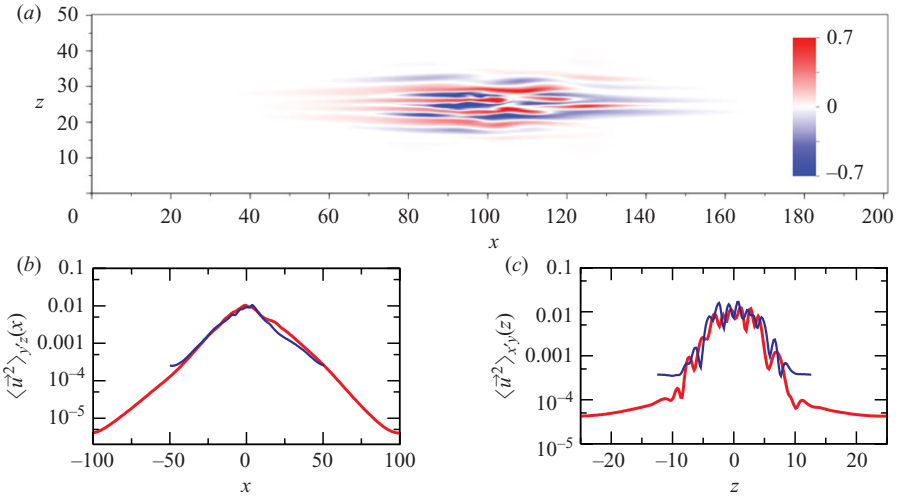

FIGURE 5. Localized turbulence seed at $Re = 400$. (*a*) The streamwise velocity in the $y = 0$ plane, emphasizing the streaky structures. in space and energy, and their fairly slow dynamics. The bottom frames highlight the localization in downstream (*b*) and spanwise (*c*) directions, by showing the energy averaged over the transverse directions. Shown are two results for two different box sizes: the central parts are similar and the larger boxes allow to follow the drop in energy further down. Note that the localization is exponential in the downstream direction and faster than exponential in the spanwise direction.

shows a streaky structure and combines the localization features observed in long but narrow and in short but wide domains: it is exponentially localized in streamwise direction (figure 5*b*) and super exponentially in spanwise direction (figure 5*c*). The overlap of the data shows that both spatial extensions and energy distributions are dynamically selected and independent of the size of the computational domain.

The fully localized edge state is not stationary or a travelling wave but shows chaotic temporal and spatial variations. As for the edge states identified in short segments of pipe flow (Schneider & Eckhardt 2006; Schneider *et al.* 2007), the mild chaotic variations can be clearly distinguished from turbulence because of their limited variability in space and energy, and their fairly slow dynamics.

The significance of the localized edge state lies in their finite size which defines the length, width and topology of marginally self-sustained perturbations. They are the smallest self-sustained structures away from the laminar profile and are critical in the sense that weaker perturbations will decay and stronger ones will increase to become turbulent. In the full state space of the system it is their stable manifold that separates laminar from turbulent dynamics. Interestingly, the size of this edge state is also very close to the minimal spot size required to stimulate growth at constant front velocity determined experimentally in (Tillmark & Alfredsson 1992): their figure 9 shows linear growth for spots with a half widths of 10 and a length of 25.

The dynamical relevance of these localized edge states for the transition is further clarified in figure 6 where the evolution from an edge state into a turbulent spot is presented. As the flow becomes turbulent the time traces of the spatial extension (length and width) and of the energy density stored in the perturbation field reveal two stages of the transition process: First, the energy increases while maintaining the size of the spot, and only once the interior has reached turbulence level does it start to grow in width and length. Thus, the structure has to become turbulent locally before it

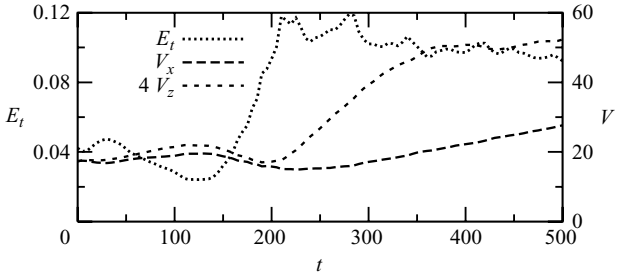

FIGURE 6. Mean amplitude E_t, height and width characterized by the variances V_x and V_z of the averaged energy distribution of a spot near the edge of chaos which swings up to turbulence. Note that the spot does not grow in size until the growth in amplitude is nearly finished.

can start to fill the domain. A similar behaviour was found for the edge states in long pipes (Mellibovsky *et al.* 2009). Incidentally, this property of the localized structures explains why they can be detected and determined by monitoring the energy only: the alternative path by which energy could increase, namely by spreading in space while keeping the local energy density of the edge state constant, does not happen.

4. Conclusions

We have computed the energetically minimal self-sustained perturbations in extended plane Couette flow and shown that they are spatially localized. These states are naturally related to earlier turbulence transition studies in which localized perturbations of a fixed type were used to generate growing turbulent spots (Tillmark & Alfredsson 1992; Dauchot & Daviaud 1995). These experimental results together with the numerical studies in (Lundbladh & Johansson 1991) show that a perturbation has to exceed a critical amplitude in order to generate a constantly growing spot. Remarkably, these studies also suggest that the critical perturbations are dominated by downstream vortices of size and topology very similar to the edge state shown in figure 5. This further supports the significance of localized edge states as nuclei for the transition dynamics.

The internal dynamics of the localized edge states can be complicated: in a wide but short domain they are travelling waves (cf. figure 1) of a topology similar to the non-localized edge states found in small periodically continued domains. In a wide and long domain the critical state is temporally active but shows a very limited spatial complexity when compared to a turbulent flow field. These observations together with the two-dimensional map studied in Vollmer *et al.* (2009) suggest that the relative attractor in the edge can be as simple or as complicated as a regular attractor in the full state space.

The localization properties discussed here introduce a new length scale to the system: comparing the observations of localized critical structures in plane Couette flow and pipe flow one notes that in both cases the structures have a localization length that is much larger than the intrinsic structures of the edge states in the small domain, but that is shorter than the diameter of turbulent patches. In principle, models of front dynamics (e.g. Schumacher & Eckhardt 2001 and references therein) could help here, but their derivation starting from the Navier–Stokes equation remains a challenge.

At Reynolds numbers above 2000 Ehrenstein, Nagata & Rincon (2009) have identified a remarkable class of two-dimensional localized states. Since the present states are fully three-dimensional, the connection to them is not clear but point to complicated, symmetry dependent connections in the edge that remain to be explored.

Aspects of the spatial evolution of turbulent patches in spatially extended systems have been considered by Pomeau (1986), who suggested that the transition could have similarities to nucleation phenomena in first order equilibrium phase transitions (Becker 1966). It is well known that in such cases a sufficiently strong perturbation is needed to induce the transition from one phase to the other. For instance, water droplets in a saturated water vapour dissolve if they are too small, and grow rapidly once they are sufficiently big. The same behaviour can be observed in the localized structures discussed here: if they are too weak or too small, they decay and only if they exceed the relevant thresholds they increase and spread. Pomeau (1986) and Manneville (2009) proposed that there should be an appropriate non-equilibrium generalization of the equilibrium phase-transition problem. The localized edge states shown here seem to be this non-equilibrium equivalent of the critical size droplets, and could be important for other aspects of the spatio-temporal dynamics in large domain turbulence as well.

The work presented here is based on the diploma thesis of Daniel Marinc (2008). Parts of the results were previously presented at the Newton Institute 'Workshop on Wall bounded shear flows', Cambridge, September 8–12, 2008, the 7th ERCOFTAC SIG33 Workshop 'Open issues in transition and flow control', Genua, October 16–18, 2008 and the 7th IUTAM Symposium on Laminar-Turbulent Transition, Stockholm, June 23–26, 2009. We thank the participants of these meetings for discussion and the Deutsche Forschungsgemeinschaft for support.

REFERENCES

Barkley, D. & Tuckerman, L. S. 2005 Computational study of turbulent laminar patterns in Couette flow. *Phys. Rev. Lett.* **94**, 014502.

Becker, R. 1966 *Theorie der Wärme*, 18th edn. Springer.

Boberg, L. & Brosa, U. 1988 Onset of turbulence in a pipe. *Z. Naturforsch.* **43a**, 697–726.

Bottin, S., Dauchot, O. & Daviaud, F. 1997 Intermittency in a locally forced plane Couette flow. *Phys. Rev. Lett.* **79**, 4377–4380.

Bottin, S., Daviaud, F., Manneville, P. & Dauchot, O. 1998 Discontinuous transition to spatiotemporal intermittency in plane Couette flow. *Europhys. Lett.* **43**, 171–176.

Burke, J. & Knobloch, E. 2007 Homoclinic snaking: structure and stability. *Chaos* **17**, 037102.

Canuto, C., Hussaini, M., Quarteroni, A. & Zang, T. 1990. *Spectral Methods in Fluid Dynamics*, 2nd revised edn. Springer.

Clever, R. M. & Busse, F. H. 1997 Tertiary and quaternary solutions for plane Couette flow. *J. Fluid Mech.* **344**, 137–153.

Darbyshire, A. G. & Mullin, T. 1995 Transition to turbulence in constant-mass-flux pipe flow. *J. Fluid Mech.* **289**, 83–114.

Dauchot, O. & Daviaud, F. 1995 Finite amplitude perturbation and spots growth mechanism in plane Couette flow. *Phys. Fluids* **7**, 335–343.

Dawes, J. H. P. 2009 Modulated and localized states in a finite domain. *SIAM J. Appl. Dyn. Syst.* **8**, 909–930.

Duguet, Y., Schlatter, P. & Henningson, D. S. 2009 Localized edge states in plane Couette flow. *Phys. Fluids* **21**, 111701.

Duguet, Y., Willis, A. P. & Kerswell, R. R. 2008 Transition in pipe flow: the saddle structure on the boundary of turbulence. *J. Fluid Mech.* **613**, 255–274.

Eckhardt, B., Faisst, H., Schmiegel, A. & Schneider, T. M. 2008 Dynamical systems and the transition to turbulence in linearly stable shear flows. *Phil. Trans. R. Soc. Lond.* A **366**, 1297–1315.

Eckhardt, B., Faisst, H., Schmiegel, A. & Schumacher, J. 2002 Turbulence transition in shear flows. In *Advances in Turbulence IX* (ed. I. P. Castro, P. E. Hancock & T. G. Thomas), pp. 701–708. CIMNE.

Eckhardt, B., Schneider, T. M., Hof, B. & Westerweel, J. 2007 Turbulence transition in pipe flow. *Annu. Rev. Fluid Mech.* **39**, 447–468.

Ehrenstein, U., Nagata, M., & Rincon, F. 2009 Two-dimensional nonlinear plane Poiseuille-Couette flow homotopy revisited. *Phys. Fluids* **20**, 064103.

Emmons, H. W. 1951 The laminar-turbulent transition in a boundary layer. *J. Aeronaut. Sci.* **18**, 490–498.

Gibson, J. F. 2004 www.channelflow.org.

Grossmann, S. 2000 The onset of shear flow turbulence. *Rev. Mod. Phys.* **72** (2), 603–618.

Hof, B., Juel, A. & Mullin, T. 2003 Scaling of the turbulence transition threshold in a pipe. *Phys. Rev. Lett.* **91**, 244502.

Hof, B., Westerweel, J., Schneider, T. M. & Eckhardt, B 2006 Finite lifetime of turbulence in shear flows. *Nature* **443**, 60–64.

Itano, T. & Toh, S. 2001 The dynamics of bursting process in wall turbulence. *J. Phys. Soc. Japan* **70**, 703–716.

Knobloch, E. 2008 Spatially localized structures in dissipative systems: open problems. *Nonlinearity* **21**, T45–T60.

Koschmieder, E. L. 1993 *Bénard Cells and Taylor Vortices*. Cambridge University Press.

Landau, L. D. 1944 On the problem of turbulence. *C.R. Acad. Sci. USSR* **44**, 311–314.

Lundbladh, A. & Johansson, A.V. 1991 Direct simulation of turbulent spots in plane Couette flow. *J. Fluid Mech.* **229**, 499–516.

Manneville, P. 2009 Spatiotemporal perspective on the decay of turbulence in wall-bounded flows. *Phys. Rev.* E **79**, 025301(R).

Marinc, D. 2008 Localized edge-states in plane Couette flow. Diploma thesis, Philipps-Universität Marburg, Marburg.

Marinc, D., Schneider, T. M. & Eckhardt, B. 2009 Edge states and the transition to turbulence in shear flows. In *Laminar-turbulent transition* (ed. P. Schlatter & D. S. Henningson), pp. 253–258, Springer.

Mellibovsky, F., Meseguer, A., Schneider, T. M. & Eckhardt, B. 2009 Transition in localized pipe flow turbulence. *Phys. Rev. Lett.* **103**, 054502.

Meseguer, A. 2003 Streak breakdown instability in pipe Poiseuille flow. *Phys. Fluids* **15**, 1203–1213.

Nagata, M. 1990 Three-dimensional finite-amplitude solutions in plane Couette flow: bifurcation from infinity. *J. Fluid Mech.* **217**, 519–527.

Peixinho, J. & Mullin, T. 2007 Finite-amplitude thresholds for transition in pipe flow. *J. Fluid Mech.* **582**, 169–178.

Pomeau, Y. 1986 Front motion, metastability and subcritical bifurcations in hydrodynamics. *Physica* D **23**, 3–11.

Prigent, A., Grégoire, G., Chaté, H., Dauchot, O. & van Saarlos, W. 2002 Large-scale finite-wavelength modulation within turbulent shear flows. *Phys. Rev. Lett.* **89**, 014501.

Reynolds, O. 1883 An experimental investigation of the circumstances which determine whether the motion of water shall be direct or sinuous, and the law of resistance in parallel channels. *Phil. Trans. R. Soc. Lond.* **174**, 935–982 + 3 plates.

Schmid, P. J. & Henningson, D. S. 1999 *Stability and Transition of Shear Flows*. Springer.

Schmiegel, A. & Eckhardt, B. 1997 Fractal stability border in plane Couette flow. *Phys. Rev. Lett.* **79**, 5250–5253.

Schneider, T. M. & Eckhardt, B. 2006 Edge of chaos in pipe flow. *Chaos* **16**, 041103.

Schneider, T. M. & Eckhardt, B. 2009 Edge states intermediate between laminar and turbulent dynamics in pipe flow. *Phil. Trans. R. Soc. Lond.* A **367**, 577–587.

Schneider, T. M., Eckhardt, B. & Yorke, J. A. 2007 Turbulence transition and the edge of chaos in pipe flow. *Phys. Rev. Lett.* **99**, 034502.

Schneider, T. M., Gibson, J. F., Lagha, M., deLillo, F. & Eckhardt, B. 2008 Laminar-turbulent boundary in plane Couette flow. *Phys. Rev.* E **78**, 037301.

Schumacher, J. & Eckhardt, B. 2001 Evolution of turbulent spots in a parallel shear flow. *Phys. Rev.* E **63**, 046307.

Skufca, J. D., Yorke, J. A. & Eckhardt, B. 2006 Edge of chaos in a parallel shear flow. *Phys. Rev. Lett.* **96**, 174101.

Tillmark, N. & Alfredsson, P. H. 1992 Experiments on transition in plane Couette flow. *J. Fluid Mech.* **235**, 89–102.

Vollmer, J., Schneider, T. M. & Eckhardt, B. 2009 Basin boundary, edge of chaos, and edge state in a two-dimensional model. *New J. Phys.* **11**, 013040.

Waleffe, F. 2003 Homotopy of exact coherent structures in plane shear flows. *Phys. Fluids* **15**, 1517–1534.

Wang, J., Gibson, J. & Waleffe, F. 2007 Lower branch coherent states in shear flows: transition and control. *Phys. Rev. Lett.* **98**, 204501.

Willis, A. P. & Kerswell, R. R. 2009 Turbulent dynamics of pipe flow captured in a reduced model: puff relaminarisation and localized edge states. *J. Fluid Mech.* **619**, 213–233.